Article:

Alalo, A.M.A., Babaie, M. orcid.org/0000-0002-8480-940X, Shirneshan, A. et al. (4 more authors) (Cover date: 15 December 2022) Exergy and energy analysis during cold-start and warm-up engine operation. Fuel, 330. 125580. ISSN 0016-2361

https://doi.org/10.1016/j.fuel.2022.125580

Exergy and energy analysis during cold-start and warm-up engine operation

Ammar Mansour A Alalo [a], Meisam Babaie [b], Alireza Shirneshan [a], Timothy A. Bodisco [c],

Zoran D. Ristovski [c, d], Richard J. Brown [c], Ali Zare [a,*],

[a] School of Engineering, Deakin University, VIC, 3216 Australia

[b] School of Mechanical Engineering, University of Leeds, Leeds, United Kingdom

[c] Biofuel Engine Research Facility, Queensland University of Technology (QUT), QLD, 4000 Australia

[d] International Laboratory for Air Quality and Health, Queensland University of Technology (QUT), QLD, 4000 Australia

[*]Corresponding author: Ali Zare, ali_z4688@yahoo.com, ali.zare@deakin.edu.au

Abstract

Cold-start is an inevitable part of the daily driving operation for most vehicles. Given that exergy analysis can evaluate the sources of losses qualitatively and quantitatively using the first and second laws of thermodynamics, this study investigated the impact of engine temperature on energy and exergy parameters during engine warm-up. Using a turbocharged Cummins engine, the performance and emissions data were measured, and energy and exergy parameters were formulated from the experimental data. Engine warm-up period was divided into seven phases, including official hot-start and cold-start, and some phases which are not considered as cold-start or hot-start by regulations. This study evaluated different parameters related to energy analysis (brake power, friction mean effective pressure [FMEP], brake specific fuel consumption [BSFC] and brake thermal efficiency [BTE]), exergy analysis (fuel input exergy, exhaust heat loss, exergy destruction and exergetic efficiency) and their correlations. Results showed that as the engine warmed up, the fuel exergy, exhaust heat losses, and exergy destruction decreased by 2.3, 34.1 and 34.1%, respectively; while, the exhaust exergy loss increased by 43.5%. The FMEP and BSFC decreased by 56.7% and 14.9% as the engine warmed up, while BTE and the exergetic efficiency increased by 5.6% and 5.3%, respectively.

Keywords: cold-start, diesel engine, exergy, exergetic efficiency, exergy destruction

1. Introduction

Thermodynamic principles have been used to quantify the energy of the system in order to find the right design as per energy demand. In addition, studying exergy concept which is related to the quality of energy can improve our understanding of thermodynamic systems providing insight into the available energy of a system, which can be utilised to increase the efficiency of the whole system and therefore aid in the optimisation of energy conversion devices [1]. For this purpose, thermodynamic principles have evolved from the first law, energy balance, to the second law, which deals with the quality of energy systems. Exergy is the key to identify the irreversibility of an energy system [2, 3].

One of the most frequently used energy systems is the internal combustion engine which consumes a significant amount of fuel worldwide; therefore, any effort to increase the efficiency of this system can be rewarding. This highlights the importance of this study. In order to determine the availability of energy for an engine, exergy analysis needs to be conducted based on the working conditions of the engine. In comparison to energy analysis, which evaluates the energy of the combustion process quantitatively, exergy analysis can show internal combustion engine inefficiencies by evaluating the source of loss in the process qualitatively and quantitatively, in addition to the origins of irreversibility.

Cold-start operation occurs regularly through the daily driving schedule for most vehicles. The significance of cold-start operation was reported by Andre [4] when he studied 55 vehicles and showed that one-third of drives started and finished within the cold-start period. However, in engine combustion-related literature, most of the publications are related to hot-start, and not many articles are related to cold-start [5-8], especially when it comes to energy and exergy analysis during cold-start.

Regulations (EU Directive 2012/46/EU) define cold-start as the first five minutes from the engine start (after the engine has reached thermal equilibrium with the ambient environment) or until the coolant reaches 70 °C. Within cold-start operation, the engine working condition is not optimal due to the sub-optimal temperature standard of the lubricating oil and engine block, which affect engine performance in addition to the exhaust emissions [9-12]. Roberts et al. [5] reported that an engine cold-start operation consumes more fuel when compared to a warm engine. It was shown that fuel consumption increased by 18% when the ambient temperature decreased from 31 ℃ to -2 ℃. Clearly demonstrating the strong dependence the efficiency has on temperature. A cause of inefficiency during cold operation has been attributed to incomplete combustion during the cold-start period due to low fuel and engine temperatures which can lead to higher friction and improper atomisation and evaporation of the fuel [13]. Compared to the hot-start, higher exhaust emissions, fuel consumption, and friction losses, in addition to lower engine power, mechanical efficiency and thermal efficiency during the cold-start period, have been reported in the literature [6, 11, 14].

In addition to engine performance and emissions parameters, the impact of low engine temperature during engine cold-start and warm-up on the overall performance and efficiency of the engine can be studied by analysing the energy and exergy parameters. In order to investigate engine performance, different researchers have performed energy and exergy analyses [15-19]. However, most studies in the literature considered the energy and exergy analyses during hot-start engine operation only. Furthermore, most diesel engine exergy studies are focussed on the influence of alternative fuels. For example, Meisami and Ajam [20] investigated the effect of castor oil biodiesel on brake thermal and exergetic efficiencies. Similarly, several fuels have been studied from an exergy perspective by Odibi et al. [21].

Cold-start is an inevitable part of the daily driving operation for most vehicles, especially in cities. Given that exergy analysis can evaluate the sources of losses in the process qualitatively and quantitatively, there is a need in the literature to study engine cold-start and warm-up operation from energy and exergy perspectives due to the significance and importance of this frequent engine operation. Based on energy and exergy principles, this study investigates the impact of engine temperature on a wide range of energy and exergy parameters during the official cold-start and hot-start periods based on regulations. This study can potentially show that the period in which the engine operation parameters (including performance and emissions) are negatively affected is significantly longer than the official cold-start boundary. To the best knowledge of the authors, no study currently published in the literature has investigated the impact of engine temperature on energy and exergy parameters during the engine cold-start and warm-up operation. This study utilises the first and second laws of thermodynamics to investigate energy quality and quantity in a diesel engine using various parameters such as fuel input exergy, brake power, exhaust heat loss, exhaust exergy loss, exergy destruction, exergetic efficiency, brake-specific fuel consumption (BSFC), brake thermal efficiency (BTE), and friction mean effective pressure (FMEP).

2. Methodology

2.1 Experimental facility

The current research has been based on both experimental and theoretical analyses of the first and second laws of thermodynamics. The experiments were conducted on a turbocharged, common-rail, six-cylinder after-cooled Cummins diesel engine, specified in Table 1 [22, 23]. In order to control the engine load, an electronically controlled hydraulic dynamometer was coupled with the engine.

Table 1: The experimental engine specification

Model	Cummins ISBe220 31
Cylinders	6 in-line
Capacity	5.9 L
Aspiration	Turbocharged
Dynamometer type	Hydraulic
Fuel injection	High-pressure common rail
Bore × Stroke	102 × 120 (mm x mm)
Maximum torque	820 Nm @ 1500 rpm
Maximum Power	162 kW 2500 rpm
Compression ratio	17.3:1

A schematic diagram of the test setup used in this study for the engine research in this work is shown in Figure 1.

In order to measure the gaseous emissions from the engine, CAI-600 CLD NO/NOx and CAI-600 CO_2 analysers were utilised. HC, O_2, and CO were measured by a Testo 350XL analyser. To measure CO_2, a SABLE CA-10 was used; the measurements from this instrument were also used to calculate the dilution ratio. The exhaust emissions were passed through a dilution tunnel prior to the measurement of the particulate matter with a DustTrak II Aerosol Monitor 8530 and a DMS500 MKII. The accuracy of the measurement instruments is shown in Table A1 in Appendix.

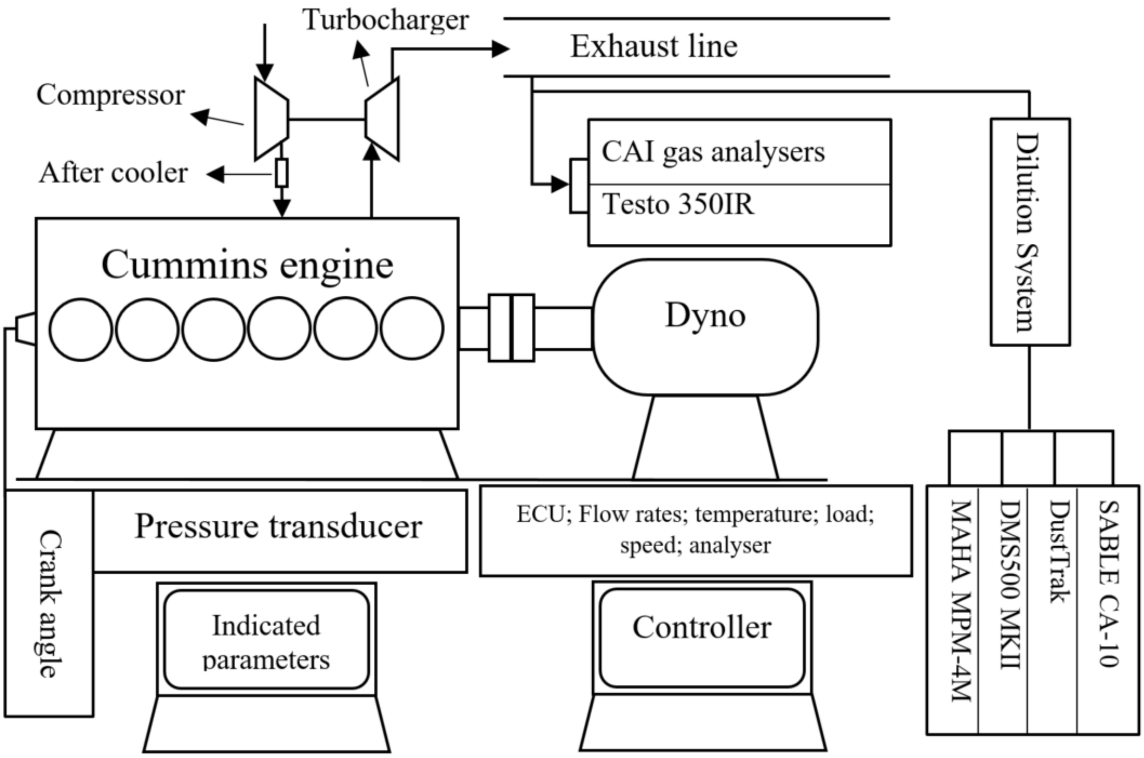

Figure 1: Schematic diagram of the test setup used in this study

2.2 Fuel properties

Commercial diesel from Caltex in Australia was utilised in this study. Table A2 in Appendix shows the fuel properties measured in an accredited laboratory using standard methods. These properties were used to develop the combustion equation in this study.

2.3 Test matrix

Regarding the cold-start experiment, the majority of research publications utilised standard driving cycles (e.g. WLTC or NEDC) and analysed the cycle's cold-start part, comparing it to the hot-start section. These driving cycles include abrupt speed/load variations [24, 25], which adds more variables to the analysis and consequently can complicate and limit the investigation of the pure effect of engine temperature on energy quality and quantity parameters. In internal combustion engines, the quality and quantity of energy depend on the operating condition, including engine load, speed and temperature. Given that the engine cold-start is an unsteady process, a constant speed and load were chosen in this study to limit the variables as much as possible and better analyse the effect of engine temperature. During the experiment, the data were collected with the highest sampling frequency—at least one Hz, depending on the type of equipment—to trace the unsteady process. And for the analysis, data were averaged over each phase (2 minutes) to include the thermal inertia. In this study, the first law of thermodynamics is used for all energy-related processes to develop the energy equations for the diesel engine energy analysis. The whole engine is the control volume, the fuel energy is considered as the input, and power is the output. And it also considers losses such as friction losses and exhaust heat loss.

The rationale for choosing 25% engine load among the particular loads of 25, 50, 75, and 100% was to replicate real-world conditions of the cold-start [26, 27]. This has been seen in standard driving cycles such as WLTC, which is developed based on actual driving data. In WLTC, the first part of the cycle is known as the low phase and is specified as the cold-start phase. For example, the average speed through the 4 phases of the WLTP class 3 cycle are 25.7, 44.5, 60.7 and 94 kph. Therefore, a 25% engine load has been selected to replicate real-world conditions.

2.4 Experiment

Cold-start preconditioning (EU Directive 2012/46/EU) was conducted to ensure that the experiment was conducted as per the regulation. This includes running the engine for an hour and turning it off to be soaked at the ambient temperature for 12 hours of natural soaking (or

6 hours forced-cooled). Before each test, the coolant and oil temperatures were checked and measured to be 23 ± 3 °C.

The cold-start duration is defined in the EU Directive of 2012/46/EU regulation, and according to that, the cold period is either the first 5 minutes after the engine start operation or once the coolant temperature reaches from ambient value to the 70 °C. It can be shown in Figure 2 that the coolant and oil temperatures increase in this period after ignition, which shows that the engine temperature is not optimum. The figure also shows that the lubricating oil temperature increases after the defined cold-start period and also when the coolant temperature is optimal. This lag between the coolant and oil temperatures indicates that the engine temperature is not optimal for some time after the cold-start period. The impact of this lag on engine performance and emission parameters has been investigated by some researchers [7, 14], showing that there are some phases after the defined cold-start phase, before the engine is fully warmed-up, which need to be investigated.

Figure 2 also has the start of injection data. The injection strategy is commanded by the ECU, and it can be seen that once the engine temperature reaches 65 °C, the start of injection increases to 361 from 353 crank angle degrees. In order to improve the analysis of the effect of engine temperature, this study divided the engine warm-up period into 7 phases, each 2 minutes. Phase 1 and 2 (the first 4 minutes in which the coolant temperature is lower than 70 °C) represent cold-start operation as per the regulation (EU Directive 2012/46/EU). Phase 7 can be considered as hot-start, given that the engine oil and coolant temperatures in this phase are optimum. The other intermediate phases cannot be considered as cold-start by the regulation, also as hot-start, given that the engine temperature within these phases is sub-optimal.

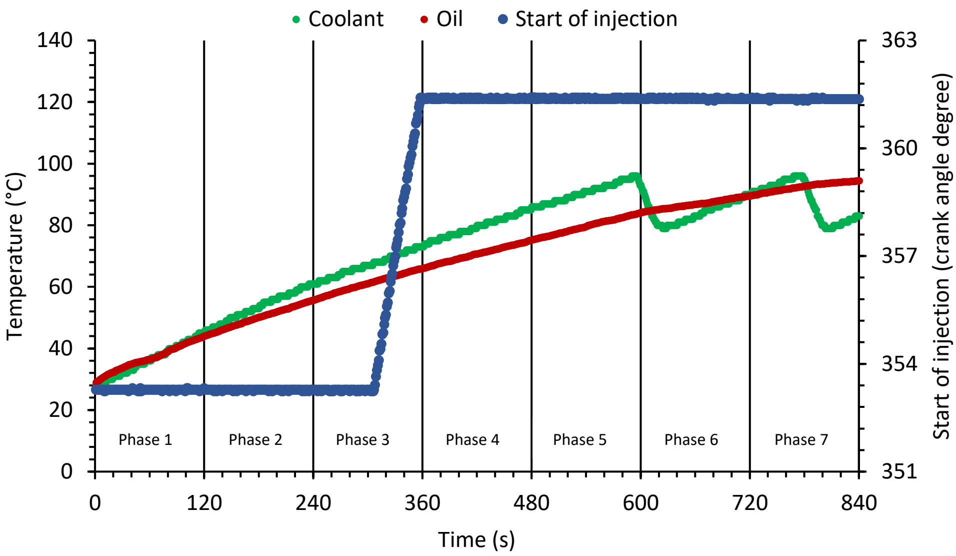

Figure 2: The variation of the temperature versus the start of injection

2.5 Energy analysis

The first law of thermodynamics is the fundamental basis for the energy analysis for all energy-related processes, and in this study, it is used to develop the energy equations for the diesel engine energy analysis. In this study:

- The whole engine, excluding the dynamometer, is in the control volume.
- The exhaust gasses from the combustion engine are considered as ideal gas mixtures.
- Due to the constant height of the engine as well as minimum variation in the gas velocity, it is assumed both kinetic and potential energies are negligible throughout the control volume.
- The magnitude of the lower heat value for fuel is determined based on the vapour saturation for the water that is exhausted from the engine manifold.

The first important parameter for the energy analysis of the engine is the total fuel input energy which is determined by fuel mass flow rate in addition to the lower heating value of the fuel (LHV), as shown:

$$\dot{Q}_f = \dot{m}_f . LHV, \tag{1}$$

where $\dot{Q}_f$ is the fuel input energy rate, $\dot{m}_f$ is the mass flow rate of the fuel in $^{kg}/_{s}$ and LHV is in $^{kJ}/_{s}$.

The next critical parameter in relation to the energy analysis that needs to be investigated is the brake power. This parameter is linked with the conducted work and shown by $\dot{W}$. This is the generated power by the engine that is calculated by torque and the engine rotational speed:

$$\dot{W} = \frac{2\pi NT}{60} (kW), \tag{2}$$

where $\dot{W}$is the brake power, T is the measured torque in kN.m and N is the engine speed (rpm).

Integrating the first law of thermodynamics and conservation of mass, the balance of the energy and mass can be written. The continuity of mass flow for incoming (i) and outgoing masses (e) can be written as:

$$\sum \dot{m}_i = \sum \dot{m}_e \qquad (3)$$

Since the first law of thermodynamics is investigated for the combustion engine. The conservation of the energy for the system can be written based on reaction and product terms of the control volume:

$$\dot{Q}_{cv} - \dot{W} = h_p - h_R, \qquad (4)$$

For the conservation of energy, where h is the enthalpy, p represents the product, R is used for reaction items, I and e are used for the inlet and exit, while cv is the control volume for the system.

Two parameters for the analysis of enthalpy are the product and reaction enthalpies h_p and h_R, and they can be written as:

$$h_p = \sum\nolimits_p n_e (h_f^0 + \Delta\bar{h})_e \qquad (5)$$

$$h_R = \sum\nolimits_R n_i (h_f^o + \Delta\bar{h})_i, \qquad (6)$$

where n_i and $n_e$are the number of moles, i and e represent inlet and exit, while h_f^0 and $\Delta\bar{h}$ are the standard enthalpy and enthalpy change.

In order to obtain the enthalpies for the energy calculation, the combustion equation should be used in which the theoretical amount of air is taken into account for that measurement. The combustion equation is written as:

$$C_xH_yO_z + \left(x + \frac{y}{4} - \frac{z}{2}\right)(O_2 + 3.76N_2) \rightarrow xCO_2 + \frac{y}{2}H_2O + 3.76\left(x + \frac{y}{4} - \frac{z}{2}\right)N_2 \tag{7}$$

The values for x, y, and z are determined based on the fuel type, and then the fuel enthalpy is determined for the rest of the calculation:

$$(h_f^o)_{Fuel} = x(h_f^o)_{CO_2} + 0.5y(h_f^o)_{H_2O} + (3.76x + 0.94y - 1.88z)(h_f^o)_{N_2} + L\bar{H}V \tag{8}$$

The variation of the enthalpy is utilised to determine the product and reaction enthalpies, as shown in Equation 9 [28]:

$$\Delta\bar{h} = \bar{h}(T) - \bar{h}(T_{ref}) \tag{9}$$

The change in heat released from the fuel in the standard situation will represent the lower heating value which is shown in Equation (9). T_{ref} is the standard reference temperature at $T_{ref} = 25°\text{C}$ in addition to $P_{ref} = 1\ atm$. By consideration of the standard reference condition for the analysis, the requirement of the calculation for the input energy is redundant. The variable T is the exhaust temperature which is determined through the experiment via installed sensors in the engine on the reaction and product sides. The heat loss through the engine can be measured via the energy balance as:

$$\dot{Q}_{exh} = \dot{m}_f . LHV - \left(\dot{W} + \left|\dot{Q}_{CV}\right|\right), \tag{10}$$

where, $\dot{Q}_{exh}$ is the heat loss through the exhaust.

The key parameters for the energy analysis of the engine are BTE and BSFC, which can be determined as per Equations 11 and 12:

$$BTE = \frac{\dot{W}}{\dot{Q}_f} \tag{11}$$

$$BSFC = \frac{\dot{m}_f}{\dot{W}} 3600 \tag{12}$$

By having the above parameters, the engine's performance for any fuel, such as diesel, can be determined. The fuel consumption for the engine during the working condition can be represented with the above parameters which are discussed in the following.

2.6 Exergy analysis

In order to conduct the exergy analysis for the existing data, the conditions that have been set for the energy analysis can be utilised here, and they are valid for the exergy analysis. Similar to the previous analysis, the reference conditions are the same, and the reference temperature is $T_0 = 298.15\ K$ in addition to an atmospheric pressure of $P_0 = 1\ atm$. The balance of exergy can be written for the current control volume as:

$$\dot{E}_Q + \dot{E}_w = \sum \dot{m}_{in} e_{in} - \sum \dot{m}_{out} e_{out} - \dot{E}_{dest} \tag{13}$$

Where, $\dot{E}_Q$ is known as the total heat exergy of the flow transported via the coolant water and it is determined as follows:

$$\dot{E}_Q = \sum \dot{Q}_{cv} \left(1 - \frac{T_0}{T_{cw}}\right) \tag{14}$$

The other parameter in the exergy balance equation is the $\dot{E}_w$ which is exergy flow, and it is determined by conducted work of the system that can be determined as below:

$$\dot{E}_w = \dot{W} \tag{15}$$

The fuel chemical exergy determined by Equation 9 will be the basis of the input exergy rate, which is calculated as:

$$\sum \dot{m}_{in} e_{in} = \dot{m}_f \phi |LHV|, \tag{16}$$

Since the incoming air to the control volume has the reference temperature, the total exergy of that would be negligible. For the equation shown above, where $\dot{m}_f$ is the mass of fuel rate and the lower heating value mentioned before is the other parameter that should be determined.

The major parameter to be determined for the input fuel exergy is ϕ, the fuel chemical exergy, and it is formulated as [28]:

$$\phi = \left[1.0401 + 0.1728\frac{h}{c} + 0.0432\frac{o}{c} + 0.2169\frac{s}{c}\left(1 - 2.0628\frac{h}{c}\right)\right] \tag{17}$$

In order to obtain the molar fraction parameters, the relevant values for the diesel engine mentioned in Ref. [21] are used, and therefore, the chemical exergy of the fuel can be known. The total gas exergy can be determined as the following [28]:

$$\sum \dot{m}_{out} e_{out} = n_f (\bar{\bar{e}}_{tm} + \bar{\bar{e}}_{ch}), \tag{18}$$

The reference environment and their respective values are calculated. The two main parameters for the calculation of the total gas exergy are including as thermomechanical, $\bar{\bar{e}}_{tm}$, and chemical exergies of the fuel, $\bar{\bar{e}}_{ch}$. For the aim of the calculation, each of the parameter has been calculated accordingly [21].

$$\bar{\bar{e}}_{tm} = \sum_i a_i\left[\bar{h}_{i,r} - \bar{h}_{i,T_0} - T_0\left(\bar{s}^0_{i,T} - \bar{s}^0_{i,T_0}\right)\right] + \bar{R}T_0 \ln\frac{P}{P_0} \tag{19}$$

The chemical exergy can also be determined by Equation 20:

$$\bar{\bar{e}}_{ch} = \bar{R}T_0 \sum_i a_i\left(\ln\frac{y_i}{y_{i,00}}\right) \tag{20}$$

The two main parameters for the calculation are y_i and $y_{i,00}$ which are determined by the combustion equation and their respective values are calculated as in Ref. [21].

Therefore, the exergy destruction can be determined as:

$$\dot{E}_{dest} = \sum \dot{m}_{in}\varepsilon_{in} - \dot{E}_Q - \dot{E}_W - \sum \dot{m}_{out}\varepsilon_{out}, \tag{21}$$

, where $\dot{E}_{dest}$ is the exergy destruction.

This parameter will assist in the calculation of the exergetic efficiency (η_{ii}) which can be formulated as below:

$$\eta_{ii} = \frac{\dot{E}_W}{\dot{E}_f} = \frac{\dot{E}_W}{\dot{m}_f e_f^{ch}} \tag{22}$$

3. Results

This section first investigates energy parameters (brake power, exhaust heat loss, FMEP, BSFC and BTE), then, exergy parameters (fuel input exergy, exhaust exergy loss, exergy destruction, and exergetic efficiency) to study the system inefficiencies by evaluating the source of losses in the process qualitatively and quantitatively. The correlation between the energy and exergy parameters is also investigated to understand engine behaviour.

3.1 Energy analysis

3.1.1 Brake power

The exergy of useful work can be determined by the brake power. It can be seen from Figure 3 that the brake power has the lowest value of 32.9 kW at Phase 1 (cold-start) and increased by 14.6% when the engine temperature increased at Phase 7 (hot-start). This is similar to other studies in the literature [29]. For instance, at a constant start of injection, with the increase of engine temperature from Phase 1 to Phase 2 within the cold-start period, the brake power increases 5.7%. An increase of 3.9% can be seen while the engine warms up through Phase 4 to Phase 6 when the start of injection is constant. By comparing the intermediate phases with cold-start and hot-start phases, the impact of the sub-optimal operation on brake power can be evaluated. For instance, the brake power of Phase 4 is 5.8% lower than Phase 7, whereas it is 7.9% higher than Phase 1. The reason for this trend is the higher friction during the early stages of engine warm-up. In this experiment, as the engine warmed up, the engine speed, load and throttle position stayed constant; therefore, the input fuel flow rate did not change much. Hence, the amount of brake power increased as the friction power decreased [14, 30].

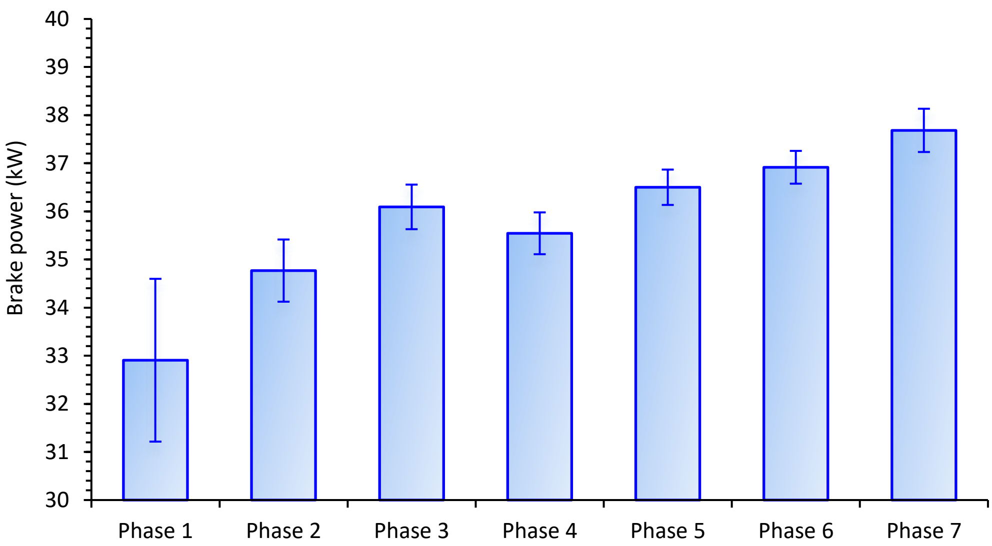

Figure 3: The variation of the brake power at 7 phases of engine warm-up

3.1.2 FMEP

It can be shown from Figure 4 that the FMEP has the highest value of 160.6 kPa at Phase 1 (cold-start), and it decreases by 56.7% at Phase 7 (hot-start). This parameter decreases with the increase of engine temperature. While the engine temperature increases through Phase 1 to Phase 2, the start of injection is constant and the FMEP decreases by 19.7%. A decrease of 19.2% can be seen when the engine warms up through Phase 4 to Phase 6 during the constant start of injection. Comparing intermediate phases with cold and hot-start phases illustrates the influence of these sub-optimal operations on FMEP. For instance, the FMEP at Phase 4 is 32.2% higher than Phase 7, while it is 42.8% less than the cold-start (Phase 1). This finding is supported by previous studies [7, 12].

The observed FMEP trend is due to the higher viscosity of the engine oil, which is because of the lower temperature in the cold phase. As the engine warms up, the engine oil temperature increases; therefore, the viscosity of engine oil decreases. This reduces the friction losses [7]. The progressive reduction in friction power (and therefore FMEP) during warm-up corresponds to an increased brake power (and therefore BMEP and useful work) during this process.

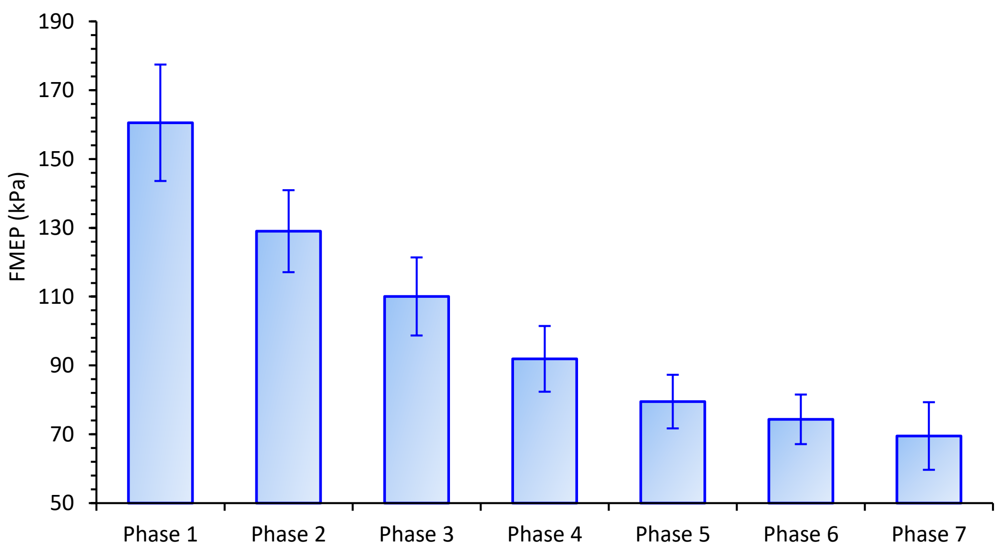

Figure 4: FMEP variation at 7 phases of engine warm-up

3.1.3 Brake specific fuel consumption

Figure 5 shows that BSFC has the highest value of 264.4 g/kWh during cold-start (Phase 1) and it decreases gradually as the engine warms up (decreased by 14.9% at Phase 7 when compared to Phase 1). BSFC at Phase 4, which is an intermediate one, is 6.1% higher than Phase 7, while it is 9.7% lower than Phase 1. This parameter decreases with the increase in engine temperature. For instance, with the constant start of injection, while the engine temperature increases from Phase 1 to Phase2, the BSFC decreases by 8.4%. This is due to higher friction losses during cold-start (therefore less generated brake power), which means that more fuel is needed at cold-start to maintain the power output [6].

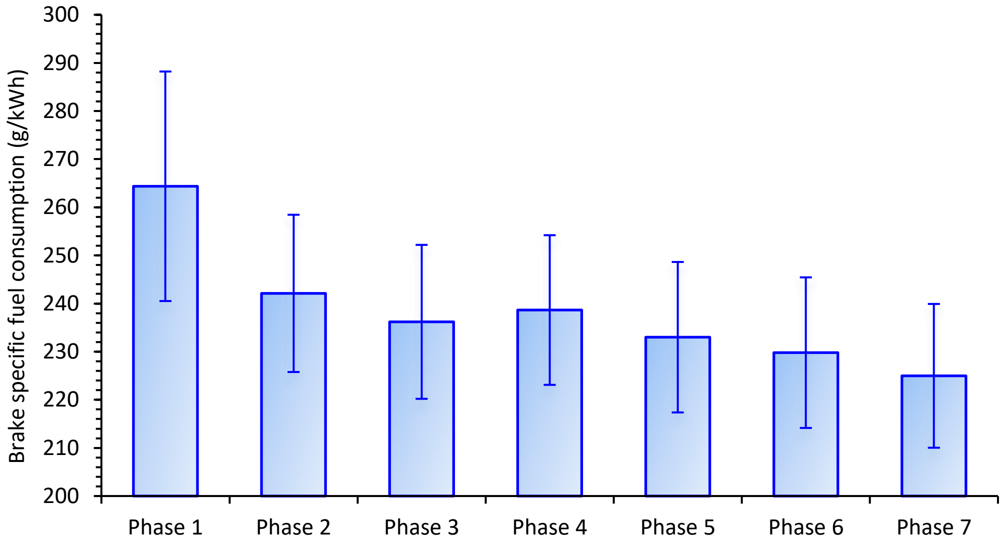

Figure 5: Brake specific fuel consumption variation at 7 phases of engine warm-up

3.1.4 Brake thermal efficiency

BTE is an index of how an engine is performing through converting the fuel energy to useful work. It can be shown from **Error! Reference source not found.** that BTE has the lowest value of 32.9% at Phase 1 (cold-start) and the highest value of 38.5% at Phase 7 (hot-start). The trend shows that with the increase of temperature, BTE increases. For instance, at a constant start of injection, with an increase in engine temperature from Phase 1 to Phase 2, BTE increases from 32.9% to 35.7%. In addition, an increase from 36.3% to 37.6% can be seen from Phase 4 to Phase 6 when the start of injection is constant. By having the comparison over the intermediate phases, the effect of sub-optimal operation can be recognised. For instance, BTE from Phase 4 is 2.1% lower than Phase 7, although it is 3.5% higher than Phase 1 or cold-start. The reason for the observed trend is due to the higher friction during cold-start; as the engine warms up, the generated brake power for the same amount of injected fuel increases; therefore, the BTE increases [6].

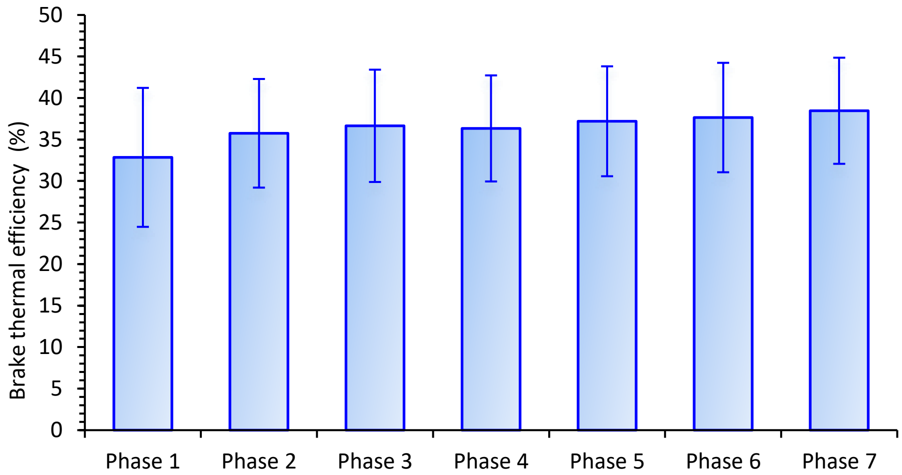

Figure 6: Brake thermal efficiency for diesel engine at 7 phases of engine warm-up

3.2 Exergy analysis

By using the second law of thermodynamics, fuel exergy conversion to work is determined for diesel engine operation. Different from fuel energy, the fuel exergy does not rely on the mass flow rate or heat value solely, but also on the chemical exergy factor. Investigating the energy balance of the system requires an exergy analysis as it can evaluate the sources of losses in the process qualitatively and quantitatively.

3.2.1 Fuel input exergy

Error! Reference source not found. shows the fuel exergy variation at 7 phases of the engine warm-up. The fuel exergy at the early stage of cold-start (Phase 1) is 107.7 kW, while Phase 7 shows that when the engine is fully warmed up, the fuel exergy decreases by 2.3%. There is a slight change (0.2%) from Phase 4 to Phase 7, whereas from Phase 1 to Phase 4 it decreased by 2.5%.

The higher fuel exergy during the cold-start phase is because of the higher required fuel to overcome the friction losses and maintain the power output. The reason for higher friction is the higher viscosity of the engine oil due to its low temperature [31].

As shown in Figure 7, the start of injection changed during Phase 3, which is the reason for the fluctuation of fuel exergy in this phase (Figure 7). This start of injection variation is because of the variation in injection strategy commanded by ECU, which advances the start of injection when the engine coolant temperature reaches 65 °C.

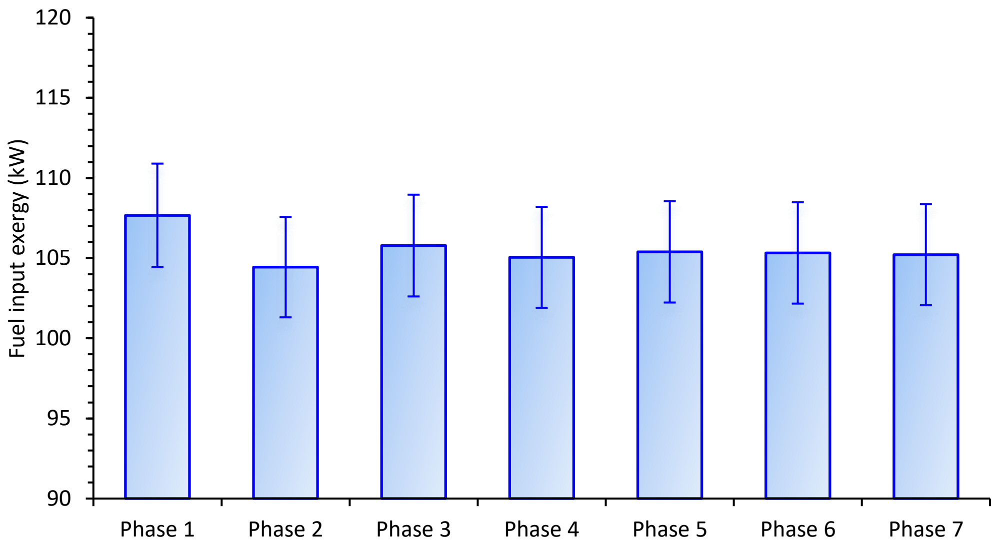

Figure 7: Fuel exergy variation at 7 phases of engine warm-up

3.2.2 Exhaust heat loss

Heat loss from the exhaust of the engine is the major source of inefficiency, which can be evaluated by looking at the ratio of exhaust energy to fuel input energy. It can be seen from Figure 8 that the exhaust heat loss has the highest value of 34.9 kW at Phase 1 (cold-start) and is reduced by 34% at Phase 7. This parameter decreases with the engine temperature. For instance, as the engine temperature increases through Phase 1 to Phase 2 within the cold period, the exhaust heat loss decreases by 24.8%. In addition, a decrease of 9.2% is seen from Phase 4 to Phase 6. By comparison of the intermediate Phases with cold-start and hot-start Phases shows the impact of these sub-optimal operations on exhaust heat loss. For example, exhaust heat loss at Phase 4 is 15.2% higher than Phase 7 and it is 28.4% lower than cold-start (Phase 1). The increasing trend of engine temperature aids the combustion, and a higher portion of the released heat will be converted to work instead of wasting through the exhaust [32]

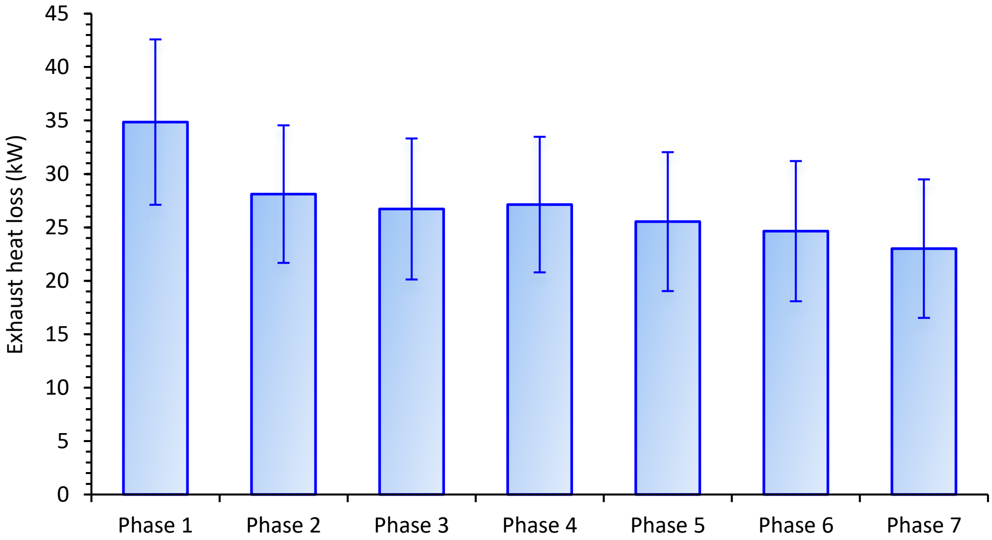

Figure 8: The exhaust heat loss from the engine at 7 phases of engine warm-up

3.2.3 Exhaust exergy loss

The exhaust heat loss can be better understood by analysing the exhaust exergy loss. It can be shown from Figure 9 that the exhaust exergy loss has the lowest value of 15.4 kW at Phase 1 (cold-start) and increased by 43.5% at Phase 7. This trend is the opposite of what has been observed in Figure 8 and confirms the importance of the exergy analysis. While the quantity of wasted heat decreases from phase 1 to 7 in Figure 8 (first law), the quality increases according to Figure 9 (second law). So, the energy losses in Phase 7 are of higher importance as it is wasting more useful work. In any improvement plan, this exergy loss should have the higher priority to be reduced or recovered, while data from Figure 8 advises otherwise. It should be mentioned that turbochargers are used to recover energy from exhaust gas.

The exhaust exergy loss of Phase 7 is the highest as most of the exhaust is hot, and there is a great potential for waste heat recovery [33]. A similar result has been reported in the literature in which the exhaust exergy loss increases with the exhaust temperature [34, 35].

As the engine temperature increases through Phase 1 to Phase 2 within the cold-start period, the exhaust exergy loss increases by 10.4%. An increase of 6.4% can also be seen when the engine warms up through Phase 4 to Phase 6. Comparing intermediate phases with cold-start and hot-start phases shows the impact of these sub-optimal operations on exhaust exergy loss. For example, the exhaust exergy loss at Phase 4 is 9.35% lower than Phase 7, while it is 23.7% higher than cold-start (Phase 1).

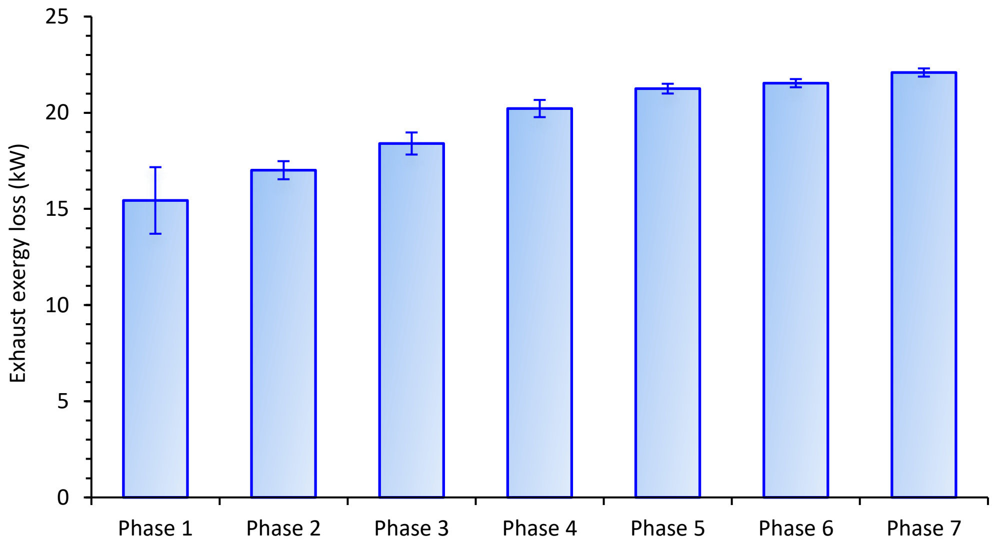

Figure 9: Exhaust exergy loss of the diesel engine at 7 phases of engine warm-up

3.2.4 Exergy destruction

With a portion of the fuel exergy converted to the brake power of the engine, the rest of the exergy is lost or destroyed in different ways. Exergy destruction is another important parameter that illustrates the irreversibility in diesel engine combustion. Exergy destruction shows the amount of energy that is destroyed and cannot be recovered. Investigation of this parameter can yield further insight into the effect of temperature on the cold-start operation.

It can be shown from Figure 10 that the exergy destruction has the highest value of 58.7 kW at Phase 1 (cold-start) and it decreases by 34.1% at Phase 7. This parameter decreases with the engine temperature increase. For example, as the engine temperature increased through Phase 1 to Phase 2 within the cold-start period, the exergy destruction decreased by 14.7%. A decrease of 12.2% can also be seen when the engine warms up through Phase 4 to Phase 6. Comparing intermediate phases with cold-start and hot-start phases, the exergy destruction at Phase 4 is 12.4% higher than Phase 7, while it is 24.8% lower than cold-start (Phase 1).

When compared to hot-start, during cold-start, a low engine temperature (less than 65℃) leads to more incomplete combustion; therefore, the irreversibility is higher, corresponding to high exergy destruction. However, as the engine warms up, the engine temperature increase and aids the combustion toward complete combustion; therefore, the level of irreversibility decreases. Consequently, it is expected to have less exergy destruction at warmed-up phases when compared to cold-start [36].

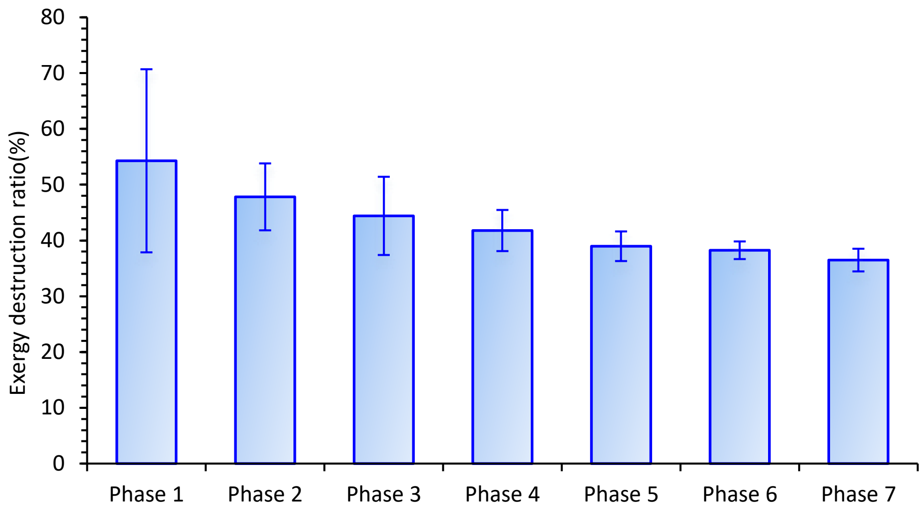

Figure 10: Exergy destruction value at 7 phases of engine warm-up

3.2.5 Exergetic efficiency

Figure 11 shows the exergetic efficiency specified as the fuel exergy converted to work at different stages of the engine warm-up. It can be seen from the figure that the exergetic efficiency has the lowest value of 30.7% at Phase 1 (cold-start) and the highest value of 36% at Phase 7. This parameter increases with the engine temperature. For example, as the engine temperature increases through Phase 1 to Phase 2 within the cold-start period, the exergetic efficiency increases from 30.7 to 33.4%. An increase from 34 to 35% can also be seen when the engine warms up through Phase 4 to Phase 6. Comparing intermediate phases with cold-start and hot-start phases, the exergetic efficiency at Phase 4 is 2% lower than Phase 7, while it is 2.3% higher than cold-start (Phase 1). The exergetic efficiency has an opposite trend to the exergy destruction. This means that there is more chance of exhaust exergy loss recovery when the engine is warmed up [37].

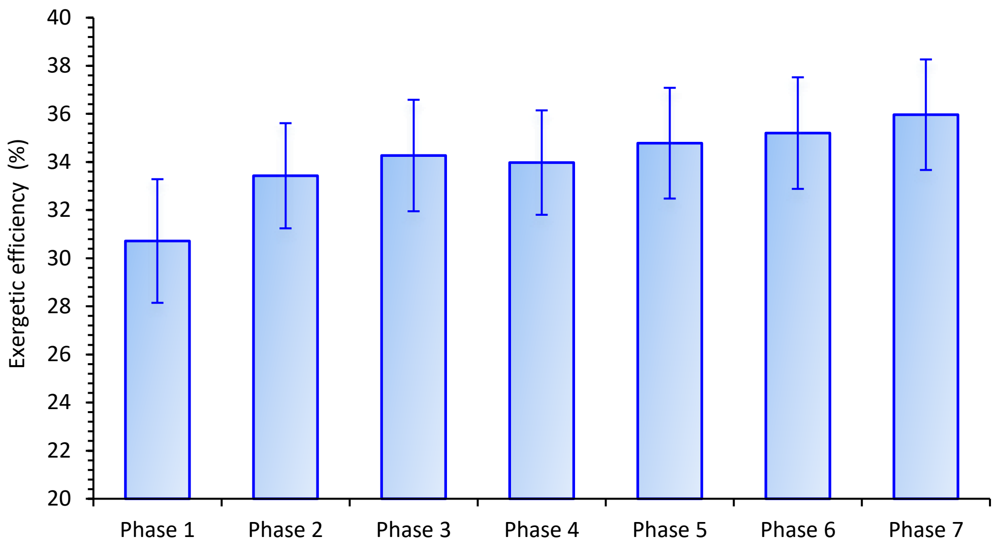

Figure 11: Exergetic efficiency variation at 7 phases of engine warm-up

3.3 Correlation between the analysis

3.3.1 Exergetic efficiency and exhaust heat loss vs brake thermal efficiency

Figure 12 shows a strong linear correlation between the exergetic efficiency and BTE. Further analysis showed that BTE has an adverse correlation with exhaust heat loss. The reason could be that as the engine temperature increases, the friction losses decrease, the BTE increases, and the heat loss through the exhaust drops [6].

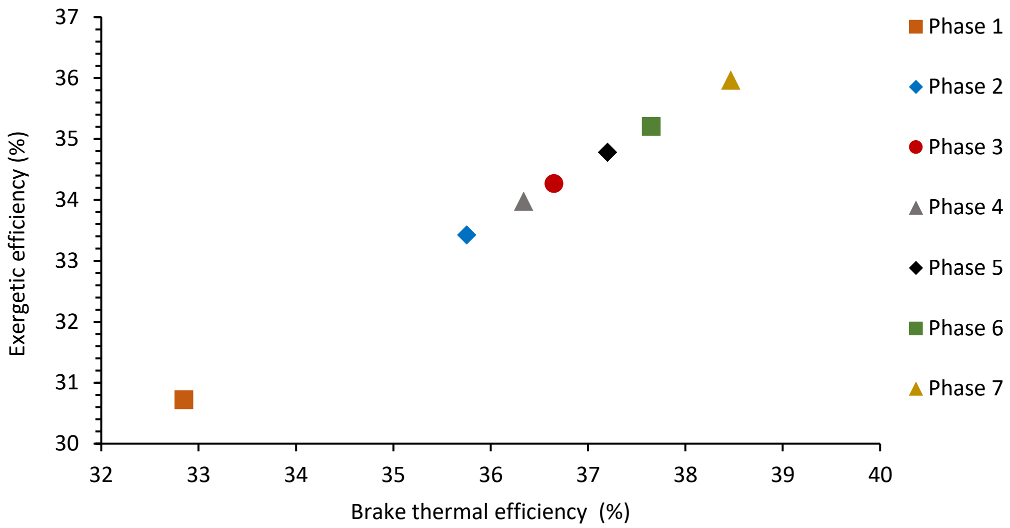

Figure 12: The variation of the exergetic efficiency and brake thermal efficiency at 7 phases of engine warm-up

3.3.2 Exhaust exergy loss vs exergy destruction

Figure 13 shows that the exergy destruction has a linear adverse correlation with the exhaust exergy loss. While the exergy destruction is the highest for the cold start, the exhaust exergy loss is at the minimum, and with the progression of the engine toward the hot phases, the exergy destruction is reduced. The engine temperature increase aids the combustion and leads to less exergy destructions (due to less irreversibility), while a hotter exhaust will leave the combustion chamber. This brings a trade-off between these two parameters with respect to exergetic efficiency, as discussed before.

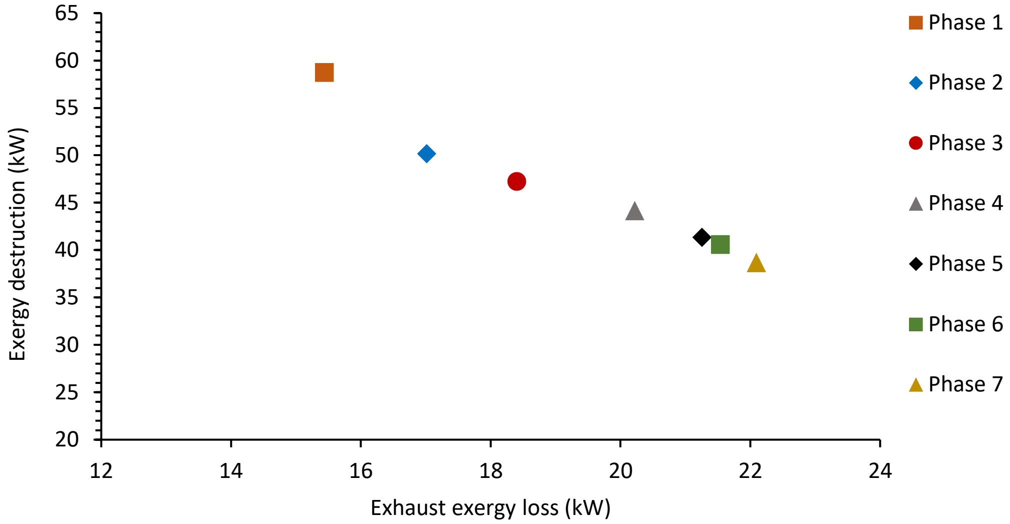

Figure 13: Exergy destruction versus exhaust exergy loss at 7 phases of engine warm-up

4. Conclusion

This study investigated the impact of engine temperature on energy and exergy principles. The equations were derived to determine the efficiency of the engine based on the energy and exergy. The importance of considering exergy analysis rather than only energy analysis was shown in this study by the opposite trend of exhaust heat loss and exhaust exergy loss. The first law found that the quantity of the wasted heat decreased from Phase 1 to 7, while the second law found that the quality increased from Phase 1 to 7, emphasising the higher priority.

And below conclusions are derived:

- Fuel exergy was maximum (107.7 kW) at cold-start and decreased by 2.3% at hot-start.
- Brake power increased by 14.6% from cold-start to hot-start.

- Exhaust heat loss and FMEP were maximum (34.9 kW, 160.6 kPa) at cold-start and minimum (34.1%, 56.7%) at hot-start.
- Exhaust exergy loss increased by 43.5% from cold-start to hot-start.
- Exergy destruction was maximum (58.7 kW) at the cold phase and decreased by 34.1% as the engine warmed up, while the exergetic efficiency was minimum (30.7%) at cold-start and increased by 5.3% as the engine warmed up.
- BSFC was maximum (264.4 g/kWh) at cold-start and decreased by 14.9% at hot-start.
- BTE increased by 5.6% from cold-start to hot-start.
- The linear relationship between the exergetic efficiency and brake thermal efficiency was observed. There was a direct linear between these parameters, while that BTE had an adverse correlation with exhaust heat loss, as the BTE increased when the heat loss through the exhaust decreased.

5. Acknowledgment

The authors acknowledge the help from Mr. Noel Hartnett from QUT and Mr. Andrew Elder from Dynolog Dynamometer Pty Ltd.

6. References

1. Boles, M. and Y. Cengel, *An Engineering Approach.* New York: McGraw-Hil l Education, 2014.
2. Borgnakke, C. and R. Sonntag, *Fundamentals of Thermodynamics (vol. 6)*. 1998, New York: Wiley.
3. Li, Y., et al., *Thermodynamic energy and exergy analysis of three different engine combustion regimes.* Applied Energy, 2016. **180**: p. 849-858.
4. André, M., *In actual use car testing: 70,000 kilometers and 10,000 trips by 55 French cars under real conditions.* SAE transactions, 1991: p. 65-72.

5. Roberts, A., R. Brooks, and P. Shipway, *Internal combustion engine cold-start efficiency: A review of the problem, causes and potential solutions.* Energy Conversion and Management, 2014. **82**: p. 327-350.
6. Zare, A., et al., *A comparative investigation into cold-start and hot-start operation of diesel engine performance with oxygenated fuels during transient and steady-state operation.* Fuel, 2018. **228**: p. 390-404.
7. Zare, A., et al., *Emissions and performance with diesel and waste lubricating oil: A fundamental study into cold start operation with a special focus on particle number size distribution.* Energy Conversion and Management, 2020. **209**: p. 112604.
8. Zare, A., et al., *Analysis of cold-start NO2 and NOx emissions, and the NO2/NOx ratio in a diesel engine powered with different diesel-biodiesel blends.* Environmental Pollution, 2021. **290**: p. 118052.
9. Lodi, F., et al., *Characteristics of Particle Number and Particle Mass Emissions of a Diesel Engine during Cold-, Warm-, and Hot-Start Operation*. 2021, SAE Technical Paper.
10. Verma, P., et al., *Soot particle morphology and nanostructure with oxygenated fuels: a comparative study into cold-start and hot-start operation.* Environmental Pollution, 2021. **275**: p. 116592.
11. Lodi, F., et al., *Combustion analysis of a diesel engine during warm up at different coolant and lubricating oil temperatures.* Energies, 2020. **13**(15): p. 3931.
12. Lodi, F., et al., *Engine performance and emissions analysis in a cold, intermediate and hot start diesel engine.* Applied Sciences, 2020. **10**(11): p. 3839.
13. Giakoumis, E.G., et al., *Exhaust emissions of diesel engines operating under transient conditions with biodiesel fuel blends.* Progress in Energy and Combustion Science, 2012. **38**(5): p. 691-715.
14. Mitchell, B.J., et al., *Engine blow-by with oxygenated fuels: A comparative study into cold and hot start operation.* Energy, 2017. **140**: p. 612-624.
15. Nabi, M.N. and M. Rasul, *Influence of second generation biodiesel on engine performance, emissions, energy and exergy parameters.* Energy conversion and management, 2018. **169**: p. 326-333.
16. Cavalcanti, E.J., M. Carvalho, and A.A. Ochoa, *Exergoeconomic and exergoenvironmental comparison of diesel-biodiesel blends in a direct injection engine at variable loads.* Energy Conversion and Management, 2019. **183**: p. 450-461.
17. Feng, H., X. Wang, and J. Zhang, *Study on the effects of intake conditions on the exergy destruction of low temperature combustion engine for a toluene reference fuel.* Energy Conversion and Management, 2019. **188**: p. 241-249.
18. Canakci, M. and M. Hosoz, *Energy and exergy analyses of a diesel engine fuelled with various biodiesels.* Energy Sources, Part B, 2006. **1**(4): p. 379-394.
19. Chaudhary, V. and R. Gakkhar, *Parametric optimisation of exergy destruction in small DI diesel engine fuelled with neem biodiesel using the Taguchi method.* International Journal of Ambient Energy, 2020. **41**(3): p. 274-284.
20. Meisami, F. and H. Ajam, *Energy, exergy and economic analysis of a Diesel engine fueled with castor oil biodiesel.* International Journal of Engine Research, 2015. **16**(5): p. 691-702.
21. Odibi, C., et al., *Exergy analysis of a diesel engine with waste cooking biodiesel and triacetin.* Energy Conversion and Management, 2019. **198**: p. 111912.

22. Zare, A., et al., *The effect of triacetin as a fuel additive to waste cooking biodiesel on engine performance and exhaust emissions.* Fuel, 2016. **182**: p. 640-649.
23. Nabi, N., et al. *Formulation of new oxygenated fuels and their influence on engine performance and exhaust emissions*. in *Proceedings of the 2015 Australian Combustion Symposium*. 2015. The Combustion Institute Australia and New Zealand Section.
24. Bodisco, T. and A. Zare, *Practicalities and driving dynamics of a real driving emissions (RDE) Euro 6 regulation homologation test.* Energies, 2019. **12**(12): p. 2306.
25. Zare, A., et al., *Engine performance during transient and steady-state operation with oxygenated fuels.* Energy & fuels, 2017. **31**(7): p. 7510-7522.
26. Zare, A., et al., *Cold-start NOx emissions: Diesel and waste lubricating oil as a fuel additive.* Fuel, 2021. **286**: p. 119430.
27. Zare, A., et al., *Particulate number emissions during cold-start with diesel and biofuels: A special focus on particle size distribution.* Sustainable Energy Technologies and Assessments, 2022. **51**: p. 101953.
28. Sayin, C., et al., *Energy and exergy analyses of a gasoline engine.* International Journal of Energy Research, 2007. **31**(3): p. 259-273.
29. Lodi, F., et al., *Gaseous and particulate emissions analysis using microalgae based dioctyl phthalate biofuel during cold, warm and hot engine operation.* Fuel, 2022. **312**: p. 122965.
30. Van, T.C., et al., *Effect of cold start on engine performance and emissions from diesel engines using IMO-Compliant distillate fuels.* Environmental pollution, 2019. **255**: p. 113260.
31. Bilgin, A., O. Durgun, and Z. Sahin, *The effects of diesel-ethanol blends on diesel engine performance.* Energy sources, 2002. **24**(5): p. 431-440.
32. Kalam, M., M. Husnawan, and H. Masjuki, *Exhaust emission and combustion evaluation of coconut oil-powered indirect injection diesel engine.* Renewable Energy, 2003. **28**(15): p. 2405-2415.
33. Ghazikhani, M., et al., *Exergy recovery from the exhaust cooling in a DI diesel engine for BSFC reduction purposes.* Energy, 2014. **65**: p. 44-51.
34. Liu, X. and R. Bansal, *Thermal power plants: modeling, control, and efficiency improvement*. 2016: CRC Press.
35. Salek, F., et al., *Energy and exergy analysis of a novel turbo-compounding system for supercharging and mild hybridization of a gasoline engine.* Journal of thermal analysis and calorimetry, 2020: p. 1-12.
36. Rakopoulos, C.D. and E.G. Giakoumis, *Second-law analyses applied to internal combustion engines operation.* Progress in Energy and Combustion science, 2006. **32**(1): p. 2-47.
37. Yao, Z.-M., et al., *Energy efficiency analysis of marine high-powered medium-speed diesel engine base on energy balance and exergy.* Energy, 2019. **176**: p. 991-1006.

7. Appendix

7.1 Instrument accuracy

Table A1 shows the accuracy of the instruments used in this study.

Table A1: The accuracy of instruments and range of gaseous emissions via time flow rate.

Measurement instruments	Type of exhaust gases	Range	Accuracy and uncertainty	Flow rate $(\mathrm{L\ min^{-1}})$
CAI-600 CO_2 Non-Dispersive Infrared (NDIR)	CO_2	0-1000/2000/3000 ppm	RESPONSE TIME (IR): T90 < 2 s-60 s Adjustable (Depending on configuration) RESOLUTION Display Five Significant Digits REPEATABLITY > 1.0% of Full Scale LINEARITY > 0.5% of Full Scale NOISE < 1% of Full Scale	0.25-2.0
CAI-600 CLD NO/NOx Chemiluminescence (CLD) Photodiode (thermally stabilized with Peltier Cooler)	NO/NOx	0-1 to 3000 ppm	RESPONSE TIME (IR): T90 < 2 s-60 s Adjustable RESOLUTION = 10 ppb NO/NOx (Display 5 significant digits) REPEATABLITY > 0.5% of Full Scale LINEARITY > 0.5% of Full Scale NOISE < 1% of Full Scale	0.3-3.0
Testo 350 XL Portable Emission Analyser	SO_2	0-5000 ppm	5% of mV	1.2
	CO	0-10,000 ppm	5% of mV	
	CO_2	0-CO_2 max	-	
	O_2	0-25%	0.8% of fV	
	NO	0-3000 ppm	5% of mV	
	NO_2	0-500 ppm	5 ppm	
	HC	0-60,000 ppm	60 ppm	
DustTrakTM II Aerosol Monitor 8530 (TSI)	PM	0.001-400 mg $\mathrm{m^{-3}}$	5%	3.0
Sable CA-10 CO_2 Analyser	CO_2	0-5% standard 0-10% optional	1% of reading	5-500 $\times$ 10^{-3})

7.2 Fuel properties

Table A2 shows the fuel properties.

Table A2: Fuel type properties

METHOD	TEST	SPECIFICATION		RESULTS	UNITS
ASTM D5773	Cloud Point (D2500 equivalent)	9	max	4	deg C
ASTM D4176	Appearance @25℃	1	max	1	
ASTM D4737A	Cetane Index (Calculated)	46	min	53.3	
ASTM D4052	Density @ 15 deg C	0.820-0.850		0.8381	deg C
ASTM D2624	Temperature at time of measurement	Report		23.1	deg C
ASTM D2624	Conductivity	80	min	386	pS/m
ASTM D86	FBP	Report		358.3	deg C
ASTM D1500	Colour (ASTM)	2.0	max	L1.0	
ASTM D482	Ash	100	max	1	mg/kg
ASTM D4530	Carbon Residue (10% Bottoms)	0.20	max	0.01	mass%
ASTM D2274	Oxidation Stability	25	max	3	mg/L
ASTM D445	Viscosity @ 40 deg C	2.0-4.5		2.638	Sq.mm/sec
ASTM D130	Copper Corrosion (3 Hrs @ 50 deg C)	1	max	1a	kg/L
ASTM D93	Flash Point	64.0	min	71	deg C
IP 387	Filter Blocking Tendency	1.41	max	1.00	
Declaration	Lubricity Additive-Lubruzol 539M	Note 2		130	mg/kg
IP 450	Lubricity (wsd) 1.4) @ 60 ℃	0.460	max	0.406	mm
ASTM D7039	Sulfur (Total)	10	max	5.9	mg/kg
Declaration	Additives (other)	Report		0.0	mg/L
ASTM D2709	Water and Sediment	0.05	max	0	vol%
ASTM D6591	Aromatics	15	min	29.8	mass%
Calculated	Static dissipator content – stadis 450	7	max	3	mg/L
ASTM D6591	Polyaromatic Hydrocarbons	11.0	max	4.6	mass%
ASTM D974	Acid Number (Total)	0.30	max	0.04	mg KOH/g
ASTM D974	Acid Number (Strong)	Nil		0.00	mg KOH/g
ASTM D86	95% Recovered	360	max	347.8	deg C
ASTM D86	90% Recovered	Report		332.0	deg C
ASTM D86	50% Recovered	Report		272.8	deg C
ASTM D86	10% Recovered	Report		223.2	deg C

7.3 Energy and exergy distribution

Figure A1 shows the variation of energy and exergy distribution within the 7 phases of the engine warm-up.

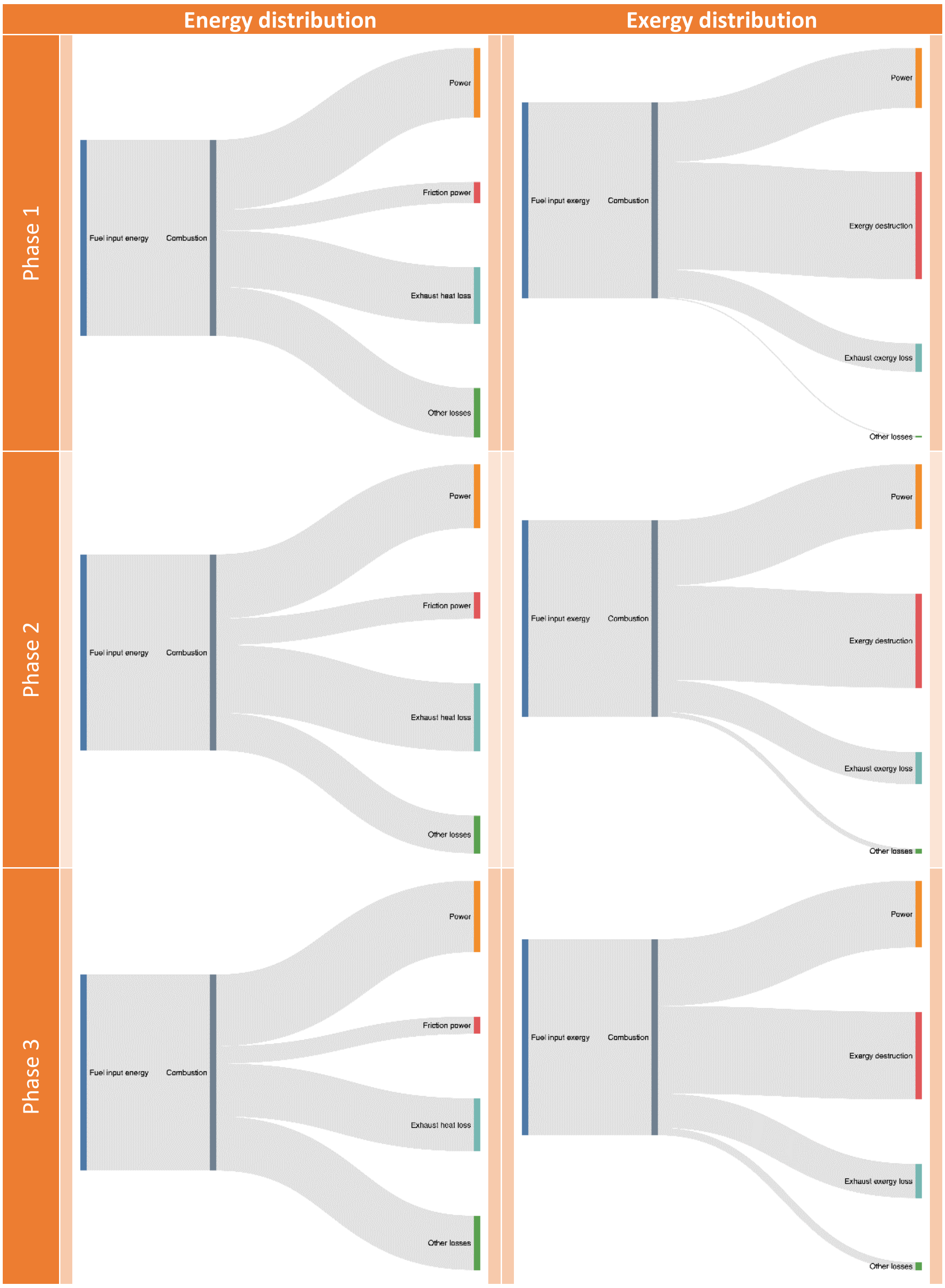

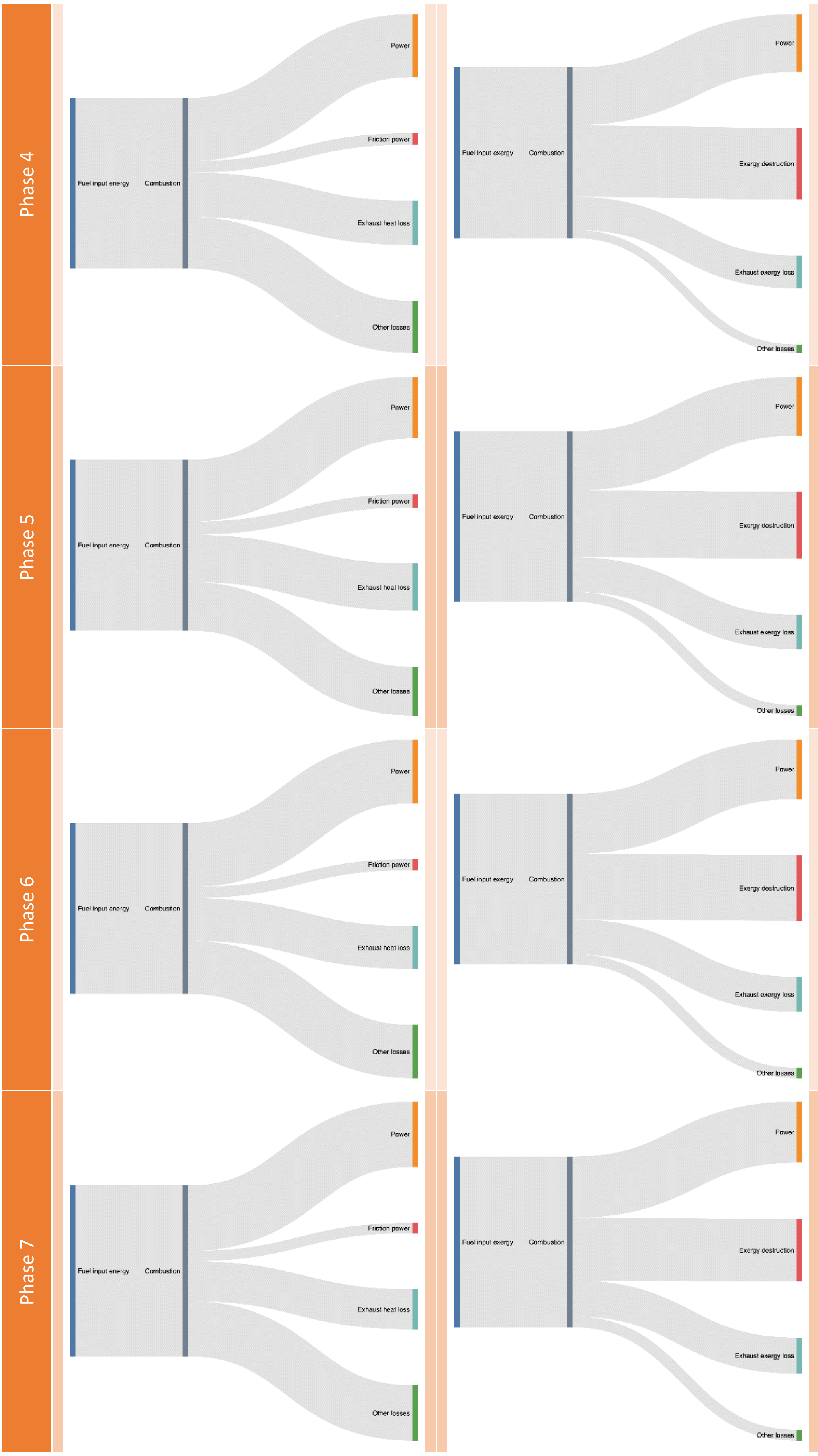

Figure 14: Energy and exergy distributions within the 7 phases of the engine warm-up

As seen in energy distribution, the share of friction power decreases within the engine warm-up period. The reason is that the increasing trend of the engine oil temperature, which reduces the viscosity of the engine oil, decreases the friction. It can also be seen that while the exhaust heat loss decreased as the engine warms up (explained in Section 3.2.2), the exhaust exergy loss increased. This shows the importance of the exergy analysis because it can be seen that as the quantity of wasted heat decreases (first law), the quality also decreases (second law). This means that the energy losses when the engine is warmed up can waste more useful work when compared to cold-start. This shows the importance of exergy losses analysis (as explained in Section 3.2.3). In exergy distribution, it can be seen that the exergy destruction decreases as the engine temperature increases. The reason is that the low engine temperature during cold-start leads to more incomplete combustion, therefore to higher irreversibility and higher exergy destruction; while, the increasing engine temperature trend aids the combustion toward complete combustion leading to lower irreversibility and lower exergy destruction.